Available online at www.sciencedirect.com
ScienceDirect
Ceramics International 35 (2009) 111–115
CERAMICS INTERNATIONAL
www.elsevier.com/locate/ceramint

Piezoelectric and dielectric properties of $(Bi_{0.5}Na_{0.5})_{0.94}Ba_{0.06}TiO_3$–$Ba(Zr_{0.04}Ti_{0.96})O_3$ lead-free piezoelectric ceramics

Zhiwu Chen [a], Jianqiang Hu [b,*]

[a] *School of Materials Science and Engineering, South China University of Technology, Guangzhou 510640, China*
[b] *School of Chemical Science, South China University of Technology, Guangzhou 510640, China*

Received 28 June 2007; received in revised form 16 July 2007; accepted 29 September 2007
Available online 15 January 2008

Abstract

Lead-free piezoelectric ceramics of $(1 - x)(Bi_{0.5}Na_{0.5})_{0.94}Ba_{0.06}TiO_3$–$xBa(Zr_{0.04}Ti_{0.96})O_3$ (abbreviated as BNBT–BZT100x, wherein x from 0 to 10 mol%) were fabricated. We have studied effects of amount of BZT content on the electrical properties and microstructures. X-ray diffraction analysis indicates that a solid solution is formed when BZT diffuses into the BNBT lattice, and further the crystal structure of sintered hybrid changes from rhombohedral to tetragonal symmetry along with increasing BZT content. Piezoelectric property measurements reveal that the BNBT–BZT4 ceramics has the highest piezoelectric performance, for example, the piezoelectric constant d_{33} reaches to 167 pC/N and planar electromechanical coupling factor k_p is up to 0.27. In addition, the effect of Bi_2O_3 on the electrical properties and microstructure of the BNBT–BZT4 ceramics have also been studied, and found that the doping of Bi enhances the piezoelectric properties of ceramics.

Keywords: C. Piezoelectric properties; C. Dielectric properties; Ferroelectrics

1. Introduction

Lead-free piezoelectric ceramics have attracted increasing attention because PbO in lead piezoelectric ceramics is volatile and detrimental to human health and the environment. It is well known that bismuth sodium titanate, *i.e.*, $(Bi_{0.5}Na_{0.5})TiO_3$ (abbreviated as BNT), discovered by Smolenskii et al. [1], is one of the most important lead-free piezoelectric materials with a perovskite ferroelectric. BNT shows a strong ferroelectricity with a large remanent polarization (P_r) of 38 $\mu C/cm^2$, a high Curie temperature (T_c) of 320 °C, and a high coercive field (E_c) of 7.3 kV/mm at room temperature [1–4]. However, the trade-off of this material is its high conductivity, and consequently resulting in a series of problems such as poling [5–7]. To improve its properties, some modifications on BNT composition have been performed. Previous studies indicate that BNT-based compositions modified with $BaTiO_3$ [8], $NaNbO_3$ [9], $Bi_2O_3 \cdot Sc_2O_3$ [10], $(Bi_{0.5}K_{0.5})TiO_3$ [11] or La_2O_3 [12] have better piezoelectric property and easier treatment in polling process as compared with pure BNT ceramics. Among them, $BaTiO_3$ are well-known lead-free piezoelectric materials with a tetragonal phase, and MPB (morphotropic phase boundary) compositions exist in the case of $x = 0.06$–0.07 for $(1 - x)(Bi_{0.5}Na_{0.5})TiO_3$–$xBaTiO_3$ (abbreviated as BNBT) ceramics. Moreover, the $(Bi_{0.5}Na_{0.5})_{0.94}Ba_{0.06}TiO_3$ exits on the rhombohedral side around the MPB region and shows fairy satisfactory piezoelectric response [8]. $Ba(Zr_{0.04}Ti_{0.96})O_3$ (abbreviated as BZT), as well as $BaTiO_3$, has an tetragonal symmetry at room temperature [13]. We have also reported the electrical properties of $(Bi_{0.5}Na_{0.5})TiO_3$–$Ba(Zr_{0.04}Ti_{0.96})O_3$ ceramics and proved that the solid solution of BNT and BZT have MPB between the tetragonal and rhombohedral phases [14]. Therefore, it is devisable to expect that the solid solution of $(Bi_{0.5}Na_{0.5})_{0.94}Ba_{0.06}TiO_3$ (rhombohedral) [5] and $Ba(Zr_{0.04}Ti_{0.96})O_3$ (tetragonal) [13] also have MPB, in which the ceramics has better piezoelectric properties [8,11,15]. However, studies on the BNBT–BZT systems ceramics have been rarely reported to date.

For the most important perovskite $Pb(Zr,Ti)O_3$ family, Bi_2O_3 is commonly used as an additive to improve their dielectric and piezoelectric properties [16]. Recently, Wang et al. [17] have reported the effect of Bi_2O_3 excess on the

---

[*] Corresponding author. Tel.: +86 20 87111905; fax: +86 20 87111905.
E-mail address: jqhusc@scut.edu.cn (J. Hu).

0272-8842/$34.00 © 2007 Elsevier Ltd and Techna Group S.r.l. All rights reserved.
doi:10.1016/j.ceramint.2007.09.110

properties of BNT ceramics and demonstrated that the Bi doping could enhance the piezoelectric properties of the ceramics. In the present work, $Ba(Zr_{0.04}Ti_{0.96})O_3$ as an additive was added into $(Bi_{0.5}Na_{0.5})_{0.94}Ba_{0.06}TiO_3$ ceramics according to the formula of $(1 - x)(Bi_{0.5}Na_{0.5})_{0.94}Ba_{0.06}TiO_3$–$xBa(Zr_{0.04}Ti_{0.96})O_3$ (abbreviated as BNBT–BZT100*x*, herein *x* from 0 to 10 mol%), and its content-depended effects on the dielectric and piezoelectric properties of the ceramics were investigated. Special emphasis was focused on seeking the MPB composition between BNBT and BZT systems for achieving great enhancement in the piezoelectric property. Moreover, Bi_2O_3 as a dopant was added into BNBT–BZT4 ceramics based on the formula of $0.96(Bi_{0.5+x}Na_{0.5})_{0.94}Ba_{0.06}TiO_3$–0.04BZT (abbreviated as $BNBT_{1+x}$–BZT4) and the influence of Bi-nonstoichiometry on the electrical properties and structure of the ceramics were also studied.

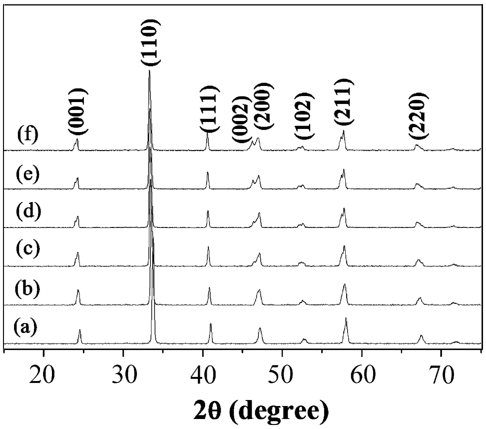

Fig. 1. X-ray diffraction patterns of BNBT–BZT100*x* ceramics with *x*: (a) 0, (b) 0.02, (c) 0.04, (d) 0.06, (e) 0.08, (f) 0.1.

2. Experimental

The preparation of BNBT–BZT100*x* (x = 0, 0.02, 0.04, 0.06, 0.08, 0.1) and $BNBT_{1+x}$–BZT4 (x = 0.02, 0.04, 0.06, 0.08, 0.1) ceramics follows a conventional mixed-oxide route. BNBT, $BNBT_{1+x}$, and BZT powders were prepared in advance. Bi_2O_3, Na_2CO_3, $BaCO_3$, and TiO_2 with >99% purities were used as starting materials of BNBT and $BNBT_{1+x}$ powder. The powders were weighed and mixed well in alcohol with zirconium balls by ball milling for 8 h. The calcination was then conducted at 800 °C for 2 h. For BZT powder, the starting materials used were $BaCO_3$, ZrO_2, and TiO_2. Calcination was conducted at 1200 °C for 2 h to get the BZT powder. Then both the BNBT (or $BNBT_{1+x}$) and BZT powders were weighted according to the formula of $(1 - x)$BNBT–xBZT (x = 0–10%) (or $0.96BNBT_{1+x}$–0.04BZT (x = 2–10%)). These powders were milled again for 6 h. After drying, it was mixed thoroughly with a PVA binder solution and uniaxially pressed into disk samples with a diameter of 20 mm and a thickness of 2 mm. The disk sample was then sintered at 1180–1230 °C for 2 h in air. The crystallite structure of the sintered sample was examined using an X-ray diffractometer (XRD, D/Max-3C, Japan) with Cu Kα radiation.

Silver paste was applied to the top and bottom surfaces of the samples as electrodes. The ceramic samples were polarized under a dc field of 7.5 kV/mm at 100 °C in a silicon oil bath for 15 min. Piezoelectric constant d_{33} of the samples were measured by means of quasistatic d_{33} meter (ZJ-3A) based on Berlincourt method. Dielectric constant $\varepsilon_{33}^T/\varepsilon_0$ was obtained by measuring the capacitance at 1 kHz using an impedance analyzer (HP4192A). Resonance measurements were performed using an impedance analyzer (HP 4294A). The electromechanical coupling factors k_p were calculated from the resonance and the anti-resonance frequencies according to Onoe's formulas [18].

3. Results and discussion

The X-ray diffraction (XRD) patterns of the BNBT–BZT100*x* ceramics are shown in Fig. 1, indicating that all the samples have pure perovskite structure and BZT has diffused into the lattice to form a solid solution. As the BZT fraction in the solid solution increases, the (1 1 0) peaks of these BNT–BZT ceramics shift monotonically to lower 2θ angel, suggesting a consecutive increase in lattice constant as a function of the BZT fraction. The X-ray diffraction patterns of these ceramics also demonstrate a phase transition from rhombohedral to tetragonal, with increasing BZT fraction. Moreover, the difference between these two structures can be seen clearly from Fig. 2 that is the XRD patterns of 44–50° in Fig. 1. Only the (2 0 0) peak is observed in the diffraction patterns for BNBT–BZT100*x* (x = 0, 0.02) ceramics, indicting that there is only a rhombohedral structure. However, (2 0 0) and (0 0 2) peaks observed in the diffraction patterns for BNBT–BZT100*x* (x = 0.1) ceramics reveal the existence of its tetragonal structure. At adding 4 mol% BZT, no obvious change in the XRD pattern was observed as compared with that of BNBT–BZT2 ceramics, but the peak at around 47° is slightly asymmetrical, featured with slightly splitting of the (2 0 0) and (0 0 2) peaks. The more BZT dopant leads to the wider separation between (2 0 0) and (0 0 2) peaks, indicating the increasing tetragonality of the lattice. Hence, it can be inferred that there should exist a rhombohedral–tetragonal

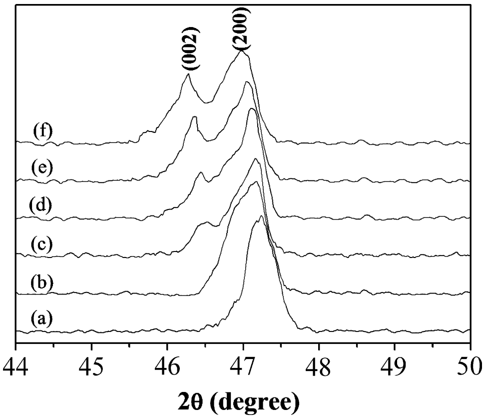

Fig. 2. X-ray diffraction patterns of BNBT–BZT100*x* ceramics in the 2θ range of 44–50° with *x*: (a) 0, (b) 0.02, (c) 0.04, (d) 0.06, (e) 0.08, (f) 0.1.

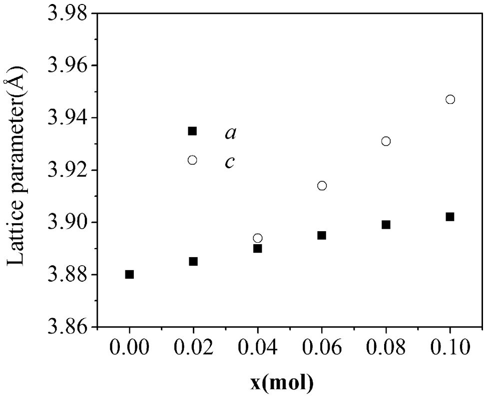

Fig. 3. Lattice parameter as a function of composition for BNBT–BZT100*x* system.

morphotropic phase boundary in the BNBT–BZT100*x* ($x = 0$–0.1) composition. Fig. 3 shows the lattice parameters of the BNBT–BZT100*x* system. In the region of the tetragonal phase, the lattice parameters *a* and *c* increases gradually with increasing the BZT content (x). The difference between *a* and *c* also increases with increasing *x*.

The interplanar distance $d_{(h,k,l)}$ of tetragonal phase is expressed as

$$d_{(h,k,l)} = \frac{a}{\sqrt{h^2 + k^2 + \left(\frac{a}{c}\right)^2 l^2}} \tag{1}$$

wherein *a* and *c* are the lattice parameters; *h*, *k*, and *l* are indices of crystallographic plane. The Bragg equation is expressed as follows:

$$2d_{(h,k,l)}\,\mathrm{Sin}\,\theta = \lambda \tag{2}$$

herein θ is Bragg angle, λ is wavelength. Combining the Eqs. (1) and (2), Sin θ can be expressed as

$$\mathrm{Sin}\,\theta = \frac{\lambda}{2}\sqrt{\frac{h^2+k^2}{a^2} + \frac{l^2}{c^2}} \tag{3}$$

From Eq. (3), we have

$$\theta_{(2\,0\,0)} - \theta_{(0\,0\,2)} = \mathrm{arc\,Sin}\left(\frac{\lambda}{a}\right) - \mathrm{arc\,Sin}\left(\frac{\lambda}{c}\right) \tag{4}$$

where $\theta_{(200)}$ and $\theta_{(002)}$ are Bragg angle for (2 0 0) and (0 0 2) crystal plane, respectively. As referred from Fig. 3, the difference between *a* and *c* increases with increasing *x*, too. Therefore, the fact that the more BZT-doped leads to the wider separation of (2 0 0) and (0 0 2) peaks is further documented through calculating Eq. (4).

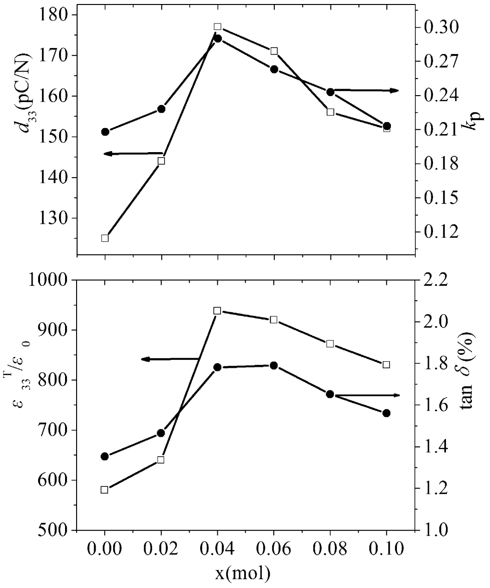

Fig. 4. Piezoelectric and dielectric properties as a function of composition for BNBT–BZT100*x* system.

Fig. 4 shows the piezoelectric and dielectric properties of the BNBT–BZT100*x* ceramics as a function of BZT amount. Coupling factor k_p increases with the amount of BZT up to 29% and then decreases with further increasing BZT amount. At 4 mol% BZT, the sample shows the optimal k_p of 29%, and variation of the piezoelectric constant d_{33} with BZT amount is almost similar to that of k_p, giving maximum d_{33} value of 177 pC/N. Dielectric constant $\varepsilon_{33}^T/\varepsilon_0$ of the samples increases with increasing BZT amount initially and reaches the maximum value ($\varepsilon_{33}^T/\varepsilon_0 = 938$) at 4 mol% BZT, and then decreases with further increasing the BZT content. Variation of the dissipation factor tan δ with increasing the BZT content is almost similar to that of $\varepsilon_{33}^T/\varepsilon_0$, but their maximum value (tan $\delta = 1.79\%$) occurs at 6 mol% of BZT. From Fig. 4, it can be seen the BNBT–BZT100*x* ceramics with a proper amount of BZT possesses improved piezoelectric and dielectric properties. Besides this, as the optimal electromechanical property occurs at 4 mol% of BZT, and combining the result of XRD, it can be concluded that the morphotropic phase boundary (MPB) should be near the BNBT–BZT4 composition.

The content-depended effect of BZT on the properties of BNBT ceramics can potentially attribute to two factors: chemical modification and microstructure influence. When BZT-doped is relatively low, chemical modification caused by dissolution of BZT into the BNBT lattice plays a major role on the properties of BNBT–BZT ceramics. Whereas the added content of BZT is increased up to a certain value enough to cause the microstructure change of the BNBT–BZT ceramics, the influence of microstructure on the properties of BNBT–BZT ceramics may become dominant. At the MPB composition (near the BNBT–BZT4 composition), the crystal structure of ceramics is considered to be a coexistence of rhombohedral and tetragonal phase [19]. As the free energy of rhombohedral phase is close to that of tetragonal phase, these two phases are easy to change each other through applying a electric field. It is helpful to promote the movement and polarization of ferroelectric active ion at this case, leading to the increase of dielectric constant $\varepsilon_{33}^T/\varepsilon_0$ and electromechanical coupling factor k_p. The increase in piezoelectric constant d_{33} at MPB composition may attribute to increase flexibility in domain wall [11]. Further increasing BZT content (>4 mol% BZT), chemical modification plays a major role on the properties of BNBT–BZT ceramics again. Our results indicate that the BNBT–BZT system, similar to PZT, have MPB, and thus make it possess stronger piezoelectric properties. That is to say, piezoelectric performance can be improved by selecting complex with different crystal phase structure and microstructure.

The X-ray diffraction pattern of BNBT$_{1+x}$–BZT4 ceramics with $x = 0$, 0.1 are shown in Fig. 5, both exhibiting a single phase perovskite structure with tetragonal symmetry and no significant differences between their diffraction patterns. Similar XRD patterns are observed from the other BNBT$_{1+x}$–BZT4 ceramics with no trace of Bi-nonstoichiometry induced second phase.

Fig. 6 gives piezoelectric and dielectric properties of the BNBT$_{1+x}$–BZT4 ceramics. It can be clearly seen from Fig. 6 that the d_{33} and k_p of the Bi-doped ceramics are higher than those of the pure BNBT–BZT ceramics. The optimized doping level is about 6 mol%, giving maximum d_{33} and k_p values of 189 pC/N and 33%, respectively. Dielectric constant $\varepsilon_{33}^T/\varepsilon_0$ of the samples gradually increases and reaches the maximum value ($\varepsilon_{33}^T/\varepsilon_0 = 998$) at $x = 0.06$ and then decreases when the Bi-doping level is continually increased. Variation of the dissipation factor tan δ with increasing x is almost similar to that of $\varepsilon_{33}^T/\varepsilon_0$, and at $x = 0.06$, the samples have the biggest tan δ value (tan $\delta = 2.39\%$).

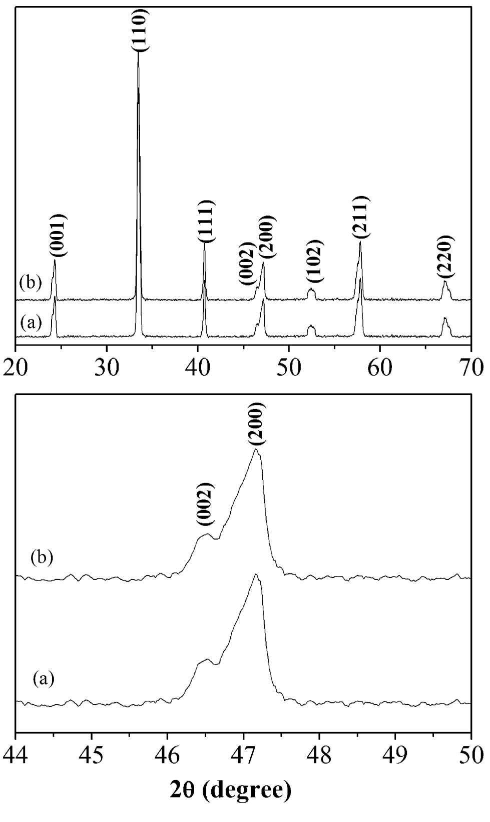

Fig. 5. X-ray diffraction pattern of BNKT$_{1+x}$–BZT4 ceramics with x: (a) 0 and (b) 0.1.

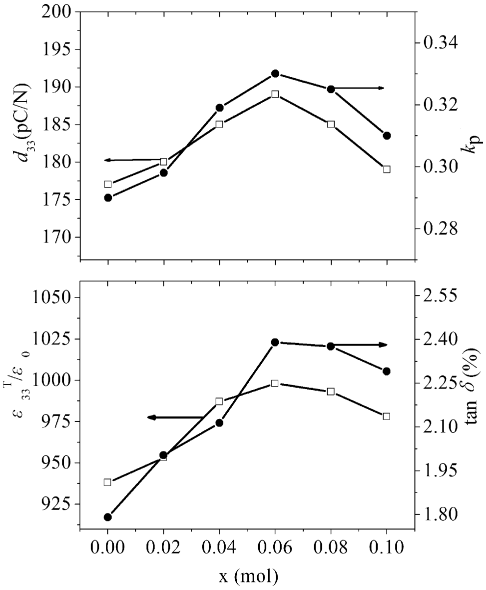

Fig. 6. Piezoelectric and dielectric properties as a function of composition for BNBT$_{1+x}$–BZT4 system.

It is supposed that BNT is A-site active in ABO$_3$ piezoelectric materials [20]. BNT-based ceramics with good piezoelectric properties can be obtained by partial substitution of A-site ions $(Bi_{0.5}Na_{0.5})^{2+}$ by Ba^{2+}, $(Bi_{0.5}K_{0.5})^{2+}$, Ba^{2+}–$(Bi_{0.5}K_{0.5})^{2+}$, and so on [20]. As A-site ions, Bi^{3+} ion, Na^+ ion, and Ba^{2+} ion is with ionic radii of 0.114 nm, 0.094 nm, and 0.142 nm, respectively, while B-site ion, Zr^{4+} and Ti^{4+} ion have ionic radii of 0.079 nm and 0.068 nm, respectively. It is the most likely that the Bi^{3+} ion can occupy A-site of BNBT6 and hence not cause any significant change of the crystallite structure if only the doping level is not too high [17]. In the Bi-doped BNBT–BZT ceramics, the doping of two Bi^{3+} ions creates one vacancy at the A site, which can relax the strain caused by reorientation of 90° domains. Therefore 90° domains in BNBT$_{1+x}$–BZT4 ceramics can be sufficiently reoriented. For piezoelectric ceramics with tetragonal symmetry, sufficient reorientation of 90° domains (strain-producing domains on switching) can improve their piezoelectric properties when specimens are poled [16]. So, as shown in Fig. 6, it is found that the doping of Bi ($x \leq 0.06$) enhances the piezoelectric properties of ceramics. Therefore, Bi_2O_3 is considered to be a soft dopant. However, further increasing Bi_2O_3 content ($x \geq 0.06$), the decreasing piezoelectric properties of ceramics may attribute to the high content of soft dopant (Bi_2O_3) [16].

The dielectric and piezoelectric properties of BNBT–BZT4, BNBT$_{1+0.06}$–BZT4, BNT–BZT6 [14], $(Bi_{0.5}Na_{0.5})_{0.94}Ba_{0.06}TiO_3$, and $Bi_{0.5}(Na_{0.8}K_{0.2})_{0.5}TiO_3$ are shown in Table 1. Among them, BNBT$_{1+0.06}$–BZT4 has the highest d_{33} and k_p, which is

Table 1
Properties of BNT–BZT6, BNT–BZT8, and BNBT6 lead-free piezoelectric ceramics

Ceramic composition	d_{33}(pC/N)	k_P(%)	$\varepsilon_{33}^T/\varepsilon_0$
BNBT$_{1+0.06}$–BZT4	189	33.0	998
BNBT–BZT4	177	29.0	938
BNT–BZT6	168	27.0	923
$(Bi_{0.5}Na_{0.5})_{0.94}Ba_{0.06}TiO_3$	125	20.8	580
$Bi_{0.5}(Na_{0.8}K_{0.2})_{0.5}TiO_3$	151	27.0	1030

promising to become the candidate of lead-free piezoelectric ceramic and find practical applications.

4. Conclusion

In summary, we have synthesized BNBT–BZT100*x* ternary system for studying the MPB between tetragonal and rhombohedral phase by a conventional ceramic sintering technique. XRD study shows that the ceramics exhibits a pure perovskite structure. And dielectric and piezoelectric property measurements reveal that the BNBT–BZT4 ceramic has relatively high piezoelectric constant d_{33} (up to 177 pC/N) and high electromechanical coupling factor k_p (up to 29%). Studies on effect of Bi_2O_3 on the electrical properties and microstructure of the BNBT–BZT4 ceramics found that all samples are a single-phase perovskite structure with tetragonal structure with no trace of Bi-nonstoichiometry induced second phase. At 6 mol% Bi doping level, the d_{33} and k_p of the ceramics both reach maximum value of 189 pC/N and 33%, respectively.

Acknowledgements

The project was funded by National Natural Science Foundation of China (no. 50702022), Natural Science Foundation of Guangdong Province (no. 07006555), Key Laboratory of Silicate Materials Science and Engineering, Wuhan University of Technology, Ministry of Education, China (SYSJJ2007-11), Key Laboratory of Low Dimensional Materials and Application Technology (Xiangtan University), Ministry of Education, China (KF0701), Key Laboratory of Specially Functional Materials and Advanced Manufacturing Technology, South China University of Technology, Ministry of Education, China.

References

[1] G.A. Smolenskii, V.A. Isupov, A.I. Agranovskaya, N.N. Krainik, Sov. Phys. Solid State 2 (1961) 2651–2654.
[2] J.V. Zrirgzds, P.P. Kapostis, T.V. Kruzina, Ferroelectrics 40 (1980) 75–77.
[3] J. Suchanicz, K. Roleder, A. Kania, J. Handerek, Ferroelectrics 77 (1988) 107–110.
[4] M.S. Hagiyev, I.H. Ismaizade, A.K. Abiyev, Ferroelectrics 56 (1984) 215–217.
[5] X.X. Wang, S.W. Or, X.G. Tang, H.L.W. Chan, P.K. Choy, P.C.K. Liu, Solid State Commun. 134 (2005) 659–663.
[6] X.P. Jiang, L.Z. Li, M. Zeng, H.L.W. Chan, Mater. Lett. 60 (2006) 1786–1790.
[7] X.X. Wang, X.G. Tang, H.L.W. Chan, Appl. Phys. Lett. 85 (2004) 91–93.
[8] T. Takenaka, K. Maruyama, K. Sakata, Jpn. J. Appl. Phys. 30 (1991) 2236–2239.
[9] T. Takenaka, T. Okuda, K. Takegahara, Ferroelectrics 196 (1997) 175–178.
[10] H. Nagata, T. Takenaka, Jpn. J. Appl. Phys. 36 (1997) 6055–6057.
[11] A. Sasaki, T. Chiba, Y. Mamiya, E. Otsuki, Jpn. J. Appl. Phys. 38 (1999) 5564–5567.
[12] A. Herabut, A. Safari, J. Am. Ceram. Soc. 80 (1997) 2954–2958.
[13] D. Hennigs, A. Schnell, J. Am. Ceram. Soc. 65 (1982) 539–544.
[14] Z.W. Chen, A.Z. Sui, Z.Y. Lu, P.A. Liu, J. Ceram. Soc. Jpn. 114 (2006) 857–860.
[15] W. Chen, Y.M. Li, Q. Xu, J. Zhou, J. Electroceram. 15 (2005) 229–237.
[16] Y.H. Xu, Ferroelectric and Piezoelectric Materials, Science Press, PR China, 1978.
[17] X.X. Wang, K.W. Kwok, X.G. Tang, H.L.W. Chan, C.L. Choy, Solid State Commun. 129 (2004) 319–323.
[18] M. Onoe, H. Jumonji, J. Acoust. Soc. Am. 41 (1967) 74–80.
[19] V.A. Isupov, Y.E. Stolypin, J. Phys. Soc. Jpn. 28 (1970) 312–317.
[20] D.M. Lin, D.Q. Xiao, J.G. Zhu, P. Yu, Appl. Phys. Lett. 88 (2006) 2901–2903.